

1 Gastrointestinal Non-motor Dysfunction in Parkinson's 2 Disease Rats with 6-hydroxydopamine

3 Xiao-Yan Feng*, Jing-Ting Yan, Xiao-li Zhang and Jin-xia Zhu

4 Department of Physiology and Pathophysiology, School of Basic Medical Science, Capital
5 Medical University, Beijing, China

6

7

8 *Corresponding authors:

9 Xiaoyan Feng, PhD

10 Department of Physiology and Pathophysiology

11 School of Basic Medical Science

12 Capital Medical University

13 No. 10 Xitoutiao, You An Men, Beijing 100069, China

14 E-mail: fengxy@ccmu.edu.cn

15 Tel: (86)10-8391-1832

16

17

18 **Short Title:** Gastrointestinal dysfunction in the 6-OHDA rats

19 **Abbreviations:** PD=Parkinson's disease; DA=dopamine; GI=gastrointestinal;

20 6-OHDA=6-hydroxydopamine; K-HS=Krebs-Hensleit solution; I_{SC} = short-circuit

21 current; UPLC-MS/MS=ultra-performance liquid chromatography tandem mass

22 spectrometry; PBST=phosphate buffer solution; TER=transepithelial resistance.

23 **Summary**

24 Parkinson's disease (PD) is a neurodegenerative disease with a progressive loss of
25 mesencephalic dopaminergic neurons of the substantia nigra (SN). To further evaluate
26 its pathophysiology, accurate animal models are needed. The current study aims to
27 verify the impact of a 6-hydroxydopamine (6-OHDA) bilateral microinjection into the
28 SN on gastrointestinal symptoms in rats and confirm that the 6-OHDA rat model is an
29 appropriate tool to investigate the mechanisms of Parkinsonian GI disorders.
30 Immunohistochemistry, digital X-ray imaging, short-circuit current, FITC-dextran
31 permeability and ultra-performance liquid chromatography tandem mass spectrometry
32 were used in this study. The results indicated that the dopaminergic neurons in SN and
33 fibres in the striatum were markedly reduced in 6-OHDA rats. The 6-OHDA rats
34 manifested reductions in occupancy in a rotarod test and increases in daily food debris
35 but no difference in body mass or daily consumption. Compared with control rats,
36 faecal pellets and their contents were significantly decreased, whereas gastric
37 emptying and intestinal transport were delayed in 6-OHDA rats. The increased *in vivo*
38 FITC-dextran permeability and decreased intestinal transepithelial resistance in the
39 model suggest attenuated barrier function in the digestive tract in the PD model.
40 Moreover, inflammatory factors in the plasma showed that pro-inflammatory factors
41 IL-1 β and IL-8 were significantly increased in 6-OHDA rats. Collectively, these
42 findings indicate that the model is an interesting experimental tool to investigate the
43 mechanisms involved in the progression of gastrointestinal dysfunction in PD.

44 **Keywords:** Parkinson's disease, gastrointestinal dysfunction, 6-hydroxydopamine

45 INTRODUCTION

46 Parkinson's disease (PD) is a chronic, progressive dopaminergic neurological disorder,
47 which is often accompanied by motor dysfunctions, such as resting tremor and rigidity,
48 and various non-motor symptoms, especially gastrointestinal (GI) dysfunctions
49 including gastroparesis, constipation and duodenal ulcer (Odin *et al.*, 2018; Sauerbier
50 *et al.*, 2017; Shen *et al.*, 2017). It has been reported that motor symptoms are realized
51 after a loss of more than 70% of the dopaminergic neurons in the substantia nigra (SN)
52 (Ferro *et al.*, 2005), but a modest reduction in dopamine content is sufficient to cause
53 GI dysfunction before the occurrence of motor disorders (Zheng *et al.*, 2014). Clinical
54 research also suggests that GI dysfunctions frequently appear in the early stages of the
55 disease or even many years before motor impairment.

56 Animal models have been acknowledged as useful and important tools to analyse the
57 pathogenic mechanisms of manifestations and potential therapeutic agents in PD
58 (Grandi *et al.*, 2018; Jakaria *et al.*, 2018). Neurotoxic agents include rotenone,
59 6-hydroxydopamin (6-OHDA), lipopolysaccharide (LPS) and 1-methyl-4-phenyl-
60 1,2,3,6-tetrahydropyridine (MPTP) (Johnson *et al.*, 2015; Marin *et al.*, 2015) and
61 dopaminergic neurotransmission drugs, such as reserpine (Shireen *et al.*, 2014) or
62 genetic manipulation (Imbriani *et al.*, 2018), have been administered to animals to
63 mimic the characteristic symptoms of PD. In all of the above cases, unilateral
64 administration of 6-OHDA to the medial forebrain bundle (MFB) (Boix *et al.*, 2015)
65 or the SN (Kim *et al.*, 2016) was the most widely used PD models. However, PD
66 affects both brain hemispheres, and GI functions are bilaterally controlled. Compared

67 to the unilateral 6-OHDA rat model, bilateral models more closely approximate the
68 real pathological situation and exclude compensation for the lesion side by the intact
69 site (Deumens *et al.*, 2002). In the present study, we aimed to verify the impact of
70 bilateral microinjection of 6-OHDA into the SN on gastrointestinal symptoms in rats
71 and confirm the 6-OHDA rat is an appropriate experimental tool to investigate the
72 mechanisms involved in the progression of GI dysfunction in PD. Metabolic
73 measurement, digital X-ray imaging, short-circuit current and FITC-dextran
74 permeability were used to determine the reproducibility of the bilateral 6-OHDA
75 model and its ability to the mimic the many physiological features of PD.

76 **METHODS**

77 **Drugs and solutions**

78 Dopamine hydrochloride, 6-hydroxydopamine hydrochloride, FITC-dextran
79 (Sigma-Aldrich, St. Louis, MO, USA), and barium meal (Kangte Biological
80 Engineering Co., Ltd, Jiangsu, China) were used in the present study. The
81 Krebs-Henseleit solution (K-HS) contained the following (in mmol/l): NaCl 117, KCl
82 4.7, MgCl₂ 6H₂O 1.2, CaCl₂ 2H₂O 2.5, NaHCO₃ 24.8, KH₂PO₄ 1.2 and glucose 11.1.
83 The solution was gassed with 95% O₂ and 5% CO₂, and HCl was used to adjust the
84 pH to 7.4.

85 **Animals and tissue preparation**

86 *Animal Care*

87 All male Sprague-Dawley rats (210-230 g) were purchased and maintained in the
88 animal facilities at the Laboratory Animal Services Center of Capital Medical

89 University. The animals were housed in a light-dark cycle of 12:12 h and provided
90 free access to food and water. All of the experiments were performed in accordance
91 with the guidelines established by the Beijing Administration Office of Laboratory
92 Animals and following the Administration Regulations on Laboratory Animals of
93 Beijing Municipality.

94 *6-OHDA Rats*

95 The methods for producing 6-OHDA rats have been previously described ([Feng *et al.*,
96 2017](#)). Briefly, the rats were received bilateral infusions of 6-OHDA (4 µg in 2 µl of
97 0.9% saline containing 0.05% ascorbic acid for each injection site) into the SN using a
98 10 µl Hamilton syringe. The control rats received 0.2% ascorbic acid/saline.

99 At 4 weeks after 6-OHDA treatment, each rat was transferred into an individual
100 metabolic cage (Ugo Basile, Gemonio VA, Italy) and observed throughout a 24 h
101 period to monitor the daily food and water consumption for one week. The food
102 residue and stool samples were collected and measured every day during the fifth
103 week. The solid matter of the stool was dried in an oven at 60°C for 12 h.

104 *Tissue Preparation*

105 The rats were killed by decapitation at the sixth week. The brains were immediately
106 removed and immersed in 4% paraformaldehyde (12 h) for post-fixation and then
107 placed in 30% sucrose (48 h) for dehydration. The brains were retained for
108 immunohistochemistry. Then, the abdominal wall was opened. The duodenum next to
109 the gastric antrum and the distal colonic segment away from the anus (approximately
110 2 cm) was quickly removed and immersed in K-HS. Each segment (1 cm) was cut
111 longitudinally along the mesenteric border and cleaned. The duodenal/colonic tissue

112 was pinned (mucosal side down) in a Sylgard-lined Petri dish to strip away the serosa,
113 muscularis and submucosa with fine forceps. The duodenal/colonic mucosa
114 preparations were obtained for *in vitro* short circuit current measurement.

115 **Immunohistochemistry**

116 The brain slices were fixed with cold acetone for 15 min, and then washed (3×5 min)
117 in 0.3% Triton X-100 phosphate buffer solution (PBST) to eliminate the residual
118 fixative. After blocking with 3% H₂O₂ and 10% goat serum (Sigma-Aldrich, St. Louis,
119 MO, USA) at room temperature for 30 min, the sections were incubated with TH
120 antibody (Mouse, 1:10000, Sigma/T1299) at 4 °C overnight. After washing in PBST
121 (3×5 min), sections of the SN were incubated with donkey anti-mouse IgG (1:1000,
122 Invitrogen/A21203) for 1 h at room temperature and then observed under a
123 fluorescence microscope (Leica DM LB2, St. Gallen, Switzerland). The sections of
124 the striatum were incubated with sheep anti-mouse IgG (1:1000, Rockland/13175) for
125 1 h at room temperature and incubated with 3, 3'-diaminobenzidine tetrahydrochloride
126 (DAB Substrate Kit for Peroxidase, Beyotime Biotechnology, Shanghai, China) for 2
127 min, stopped with water, and then placed in xylene and overlaid with a coverslip using
128 neutral resin-mounting medium.

129 **Ultra-performance liquid chromatography tandem mass spectrometry** 130 **(UPLC-MS/MS)**

131 The SN, striatum and DMV tissues were harvested from the rats at the sixth week.
132 The DA content in these tissues was measured by UPLC-MS/MS analysis, which has
133 been described elsewhere (Zhang *et al.*, 2015). Briefly, each sample was weighed and

134 homogenized in 2% aqueous formic acid. The homogenates were ultrasonically
135 dissociated with a mixture of acetonitrile/methanol/formic acid and centrifuged. The
136 supernatant was evaporated to dryness and re-dissolved with reconstitution solvent
137 followed by another round of centrifugation. The supernatant was immediately used
138 for UPLC-MS/MS analysis (Key Laboratory of Radiopharmaceuticals, Ministry of
139 Education, College of Chemistry, Beijing Normal University).

140 **Rotarod test**

141 A rotarod test was used to evaluate motor coordination by measuring the ability of a
142 rat to stay on a rotating drum. At the fifth week after 6-OHDA treatment, the rats were
143 placed on the rotarod instrument (diameter 3.75 inches, Acceler Rotarod; Jones &
144 Roberts Company, Olympia) at a fixed speed for adaptive training before testing (3-5
145 min, 3 times each day for 3 consecutive days). On the test day, the rats were trained
146 for 3-5 min until they adapted to 8 rpm/min on the rotarod. After the rats were
147 balanced, the drum was gradually accelerated until the rats fell off of the drum. The
148 time and speed to fall was recorded by a sensing platform. Each rat was given 3 trials,
149 and the mean time of the 3 trials was calculated.

150 **Gastrointestinal motility**

151 Gastric emptying was assessed using an *in vivo* digital X-ray imaging. Each animal
152 received 3 mL of a barium meal (barium sulphate) through oral gavage after fasting
153 for 20 h. The Kodak In Vivo Imaging System FX was used to obtain the gut plain
154 radiographs with a manual focus distance of 50 ± 1 cm and an exposure time of 30 s.
155 The images were recorded every 45 min after barium meal ingestion. The barium
156 sulphate content in the stomach was measured with area and greyscale. The intestinal
157 motility was measured by the total intestinal transit time, which was recorded by the

158 first stool including barium sulphate.

159 **Short-circuit current (I_{SC}) measurement**

160 The duodenal/colonic mucosa preparations were mounted between the two halves of
161 an Ussing chamber, bathed in 5 ml K-HS (37 °C) in both sides and gassed with 95%
162 O₂ and 5% CO₂. The transepithelial potential difference for each preparation was
163 measured with the Ussing chamber system (Physiologic Instruments, San Diego, CA,
164 USA; VCC MC6).

165 ***In vivo* permeability measurement**

166 The assay was slightly modified from the previously described methods ([Moussaoui](#)
167 [et al., 2016](#)). Briefly, the rats were given an oral gavage of fluorescein isothiocyanate
168 (FITC)-dextran (4.4kD) at a final dose of 600 mg/kg in PBS at 9:00 am. After 4 h, a
169 blood sample was taken from each rat by cardiac puncture. The blood was centrifuged
170 at 4 °C, 3000 ×g for 20 min, and the plasma was taken for the analysis of the
171 FITC-dextran concentration. The plasma was diluted at 1:2 with PBS, and the
172 fluorescence intensity of the diluted plasma was then measured by using a
173 fluoro-spectro photometer (Hitachi Ltd, Tokyo, Japan) with an excitation wavelength
174 of 480 nm and an emission wavelength of 520 nm. The plasma FITC-dextran
175 concentrations were calculated from standard curves generated by serial dilution of
176 FITC-dextran in control plasma.

177 **Statistical analysis**

178 The results are given as arithmetic means ± SEM; “*n*” refers to the number of rats or
179 the number of pairs. Statistical analyses included the Student’s paired or unpaired

180 *t*-test. Statistics and graphs were generated by using GraphPad Prism, version 5.0
181 (GraphPad Software, San Diego, Calif., USA). “*p*” values less than 0.05 were
182 assumed to denote a significant difference.

183 **RESULTS**

184 **Characterization of the bilateral 6-OHDA lesions**

185 Tyrosine hydroxylase (TH), which is the rate-limiting enzyme of DA synthesis, acts
186 as the most important dopaminergic marker. The results indicated that the
187 TH-immunoreactive dopaminergic neurons in SN and the fibres in the striatum were
188 significantly reduced in 6-OHDA rats (Fig. 1A). Compared to the control rats, the DA
189 contents in the SN and striatum were markedly decreased from 63.7 ± 6.9 ng/g to
190 40.4 ± 4.9 ng/g ($n=8$, $p<0.05$) and from 2270.0 ± 181.2 ng/g to 1344.0 ± 95.9 ng/g ($n=8$,
191 $p<0.001$), respectively (Fig. 1B).

192 At the fifth week after 6-OHDA treatment, each rat was transferred into an individual
193 metabolic cage to its monitor body mass and daily consumption for one week. No
194 difference in body mass (399.7 ± 5.6 g vs. 389.7 ± 6.2 g), food (30.2 ± 1.3 g vs. 29.1 ± 2.9
195 g) and water consumption (27.4 ± 1.2 g vs. 26.6 ± 1.3 g) were observed between the
196 control and the 6-OHDA rats ($n=12$, $p>0.05$). However, the rotarod test results
197 showed decreased treadmill occupancy times in 6-OHDA rats ($n=12$, $p<0.001$) (Fig.
198 1C), which suggests that the lesion of dopaminergic neurons in the SN caused motor
199 coordination and balance function disorder. As shown in Fig. 1D, the food residue
200 was detected at the bottom of the metabolic cage and collected throughout a 24 h
201 period for measurement. The increased daily food debris of 6-OHDA rats, from

202 0.3±0.1 ng/g to 3.1±0.2 ng/g ($n=12$, $p<0.001$), suggested the emergence of rigidity in
203 the PD model ($n=10$, $p<0.001$) (Fig. 1E).

204 **Gastrointestinal motility dysfunction of the 6-OHDA rats**

205 An *in vivo* digital X-ray imaging system was used to evaluate gastric emptying and
206 intestinal transit time. Following a 20 h fast, 3 mL of a barium sulphate suspension
207 was administered to each rat at room temperature. Images were recorded every 45 min
208 after barium meal ingestion. The results indicated that the gastric areas of 6-OHDA
209 rats were significantly larger than those of the control group, but gastric emptying and
210 intestinal barium meal transit were apparently slower in all images throughout the
211 experiment (Fig. 2A). After barium meal intragastric administration for 3 h, the
212 gastric areas were obviously increased from 0.69±0.06 in the control group to
213 0.96±0.06 in the 6-OHDA group ($n=7$, $p<0.01$); however, compared to the control
214 stomach content emptying of 74.11 ±4.37%, only 37.30 ±2.90% of the stomach
215 contents were emptied in the 6-OHDA rats ($n=7$, $p<0.001$) (Fig. 2B). Intestinal transit
216 is most often measured as the total intestinal transit time along the entire alimentary
217 tract and is mainly a function of propulsion in the small and large intestine. To
218 confirm the intestinal transit time, the time of the first stool including barium meal
219 was recorded. The 6-OHDA rats produced a longer transit time after barium meal
220 intragastric administration from 339±14 min to 483±26 min ($n=8$, $p<0.001$) (Fig. 2C).
221 Furthermore, the number of daily faecal pellets and the faecal content, including solid
222 matter ($n=15$, $p<0.001$) and moisture ($n=15$, $p<0.05$), were significantly decreased in
223 6-OHDA rats (Fig. 2 D-F), which indicated the impairment of GI motility.

224 **Gastrointestinal barrier dysfunction of the 6-OHDA rats**

225 The FITC-dextran concentration was determined from analysis of the standard curve
226 of dextran-FITC using a 96-well microplate fluorescence reader. Compared with the
227 control rats, the 6-OHDA rats showed increased FITC-dextran permeability from
228 $0.16 \pm 0.02 \mu\text{g/ml}$ to $0.23 \pm 0.02 \mu\text{g/ml}$ by *in vivo* measurement ($n=9$, $p<0.01$) (Fig. 3A),
229 whereas intestinal transepithelial resistance (TER) decreased from $46.36 \pm 2.82 \Omega/\text{cm}^2$
230 to $35.38 \pm 3.52 \Omega/\text{cm}^2$ ($n=12$, $p<0.05$) in the duodenal preparations and from
231 $95.19 \pm 4.88 \Omega/\text{cm}^2$ to $62.60 \pm 4.89 \Omega/\text{cm}^2$ ($n=12$, $p<0.05$) in the colonic preparations
232 (Fig. 3B), which suggested that the intestinal mucosal barrier was impaired. A link
233 between alterations in inflammatory factors and GI dysfunction, especially intestinal
234 permeability, has been reported (Netusha *et al.*, 2008). Therefore, inflammatory
235 factors in the plasma were detected. The results showed that the pro-inflammatory
236 factors IL-1 β ($n=7$, $p<0.05$) and IL-8 ($n=7$, $p<0.01$) were significantly increased, and
237 the anti-inflammatory factor IL-10 ($n=7$, $p<0.01$) was decreased in 6-OHDA rats.

238 **DISCUSSION**

239 Although the 6-OHDA rats employed in the present study did not mimic all clinical
240 and pathological symptoms of PD patients, the data in the present study provided
241 evidence that this animal model is a useful tool to investigate the mechanisms of
242 Parkinsonian GI disorders. GI dysfunction, together with sleep dysfunction, dysosmia,
243 and other dysautonomia are included in the non-motor symptoms (NMS) of PD,
244 which are key components of PD and present from the ‘pre-motor’ phase to the final
245 palliative stage (Zis *et al.*, 2015). Therefore, using the bilateral 6-OHDA model to

246 study the mechanisms involved in the progression of GI dysfunction in PD would
247 benefit the quality of life in PD patients.

248 The main neuropathological features of PD are the loss of dopaminergic neurons in
249 the SN and their projections into the caudate nucleus (Zheng *et al.*, 2011). The results
250 from immunohistochemistry and UPLC-MS/MS showed significant depression of the
251 TH-immunoreactive signalling and DA content of the SNs and striata of the 6-OHDA
252 rats. It has been reported that a direct or indirect connection may exist between the
253 SN-striatum and the DMV (Zheng *et al.*, 2011), and DA modulates the neurons in the
254 DMV, which may contribute the impaired gastric motility (Anselmi *et al.*, 2017).

255 Furthermore, activating D₁R or D₂R in the DMV can hyperpolarize or depolarize the
256 membrane potential of DMV neurons innervating the GI tract, especially those in the
257 stomach (Zheng *et al.*, 2007).

258 GI dysfunction is often considered an essential PD symptom that dominates the
259 clinical outlook for some patients and is mostly represented by gastroparesis,
260 constipation and peptic ulcers (Jiang P *et al.*, 2018; Fornai *et al.* 2016). It has been
261 found that 6-OHDA rats had enhanced expression of dopaminergic markers, which
262 suggests a significant increase of DA content in the guts of 6-OHDA rats (Tian *et al.*
263 2008). However, increased DA and reduced acetylcholine content in the gastric
264 muscularis externa lead to impaired gastric motility in 6-OHDA rats (Zheng *et al.*
265 2014). Zhang *et al.* also reported that high DA levels and upregulated D₁ receptors in
266 smooth muscle resulted in an enhanced inhibitory effect on colonic contraction in the
267 cold-restraint stress condition (Zhang *et al.* 2012). The radiological findings regarding

268 delayed intestinal transit have been previously observed in 6-OHDA unilateral
269 administration rats, which is also due to an impairment of acetylcholine release from
270 colonic myenteric neurons (Fornai *et al.* 2016). In the present study, we applied an *in*
271 *vivo* digital X-ray imaging system to confirm impaired gastric emptying and intestinal
272 transit time in 6-OHDA rats. The alterations of the enteric neurotransmitters (DA,
273 acetylcholine, nitric oxide, and vasoactive intestinal peptide) involved in the
274 regulation of intestinal motility in the 6-OHDA model suggest that central
275 dopaminergic neurodegeneration is associated with remodelling of enteric
276 neurotransmission (Pellegrini *et al.*, 2016). In contrast, the intraperitoneal
277 MPTP-lesioned mice showed a loss of dopaminergic neurons both in the SN and in
278 the gastric wall (Tian *et al.* 2008; Natale *et al.* 2010), while the MPTP-based animal
279 models showed no significant changes in gastric emptying or intestinal transit time
280 (Anderson *et al.* 2007).

281 Mucosal barrier damage with high permeability and bowel inflammation plays an
282 important role in peptic ulcer formation (Feng *et al.* 2017). Intestinal permeability can
283 be assessed *in vivo* by determining the permeability of FITC-dextran with a defined
284 molecular size in the blood plasma. TER is another common physiological index used
285 to evaluate the mucosal barrier. Our study showed that 6-OHDA rats had increased
286 FITC-dextran permeability and decreased TER in the gut, thus indicating attenuated
287 mucosal integrity (Monica *et al.* 2015). Moreover, the GI barrier can provide an
288 immune sentinel function by secreting various cytokines in the bacterial stimulation,
289 including the IL-1 family (e.g., IL-1 β , IL-18, and IL-33), IL-6, IL-8, and some

290 anti-inflammatory cytokines (e.g., IL-10 and IL-25). Studies have shown that IL-1 β
291 participates in the inflammatory responses by augmenting the infiltration of
292 neutrophils via the activation T cells and innate lymphoid cells (Sun *et al.* 2017). Our
293 results showed that 6-OHDA rats displayed a chronic intestinal disorder, which was
294 caused by an exaggerated immune response with increased pro-inflammatory factors
295 IL-1 β and IL-8 and decreased anti-inflammatory factor IL-10. Interestingly, similar
296 results have also been reported by Pellegrini et al. in that there were increased levels
297 of MDA, TNF, and IL-1 β in colonic walls isolated from 6-OHDA rats, which suggests
298 the presence of gut inflammation and oxidative stress in the colonic wall (Pellegrini *et*
299 *al.*, 2016).

300 In conclusion, our findings suggest that 6-OHDA rats would be an available PD
301 model to investigate the mechanisms involved in the progression of GI non-motor
302 dysfunctions and improve the quality of life of PD patients though drug treatment and
303 more effective assistance.

304 **ACKNOWLEDGMENTS**

305 This work was financially supported through grants from National Key Research and
306 Development Program (2016YFC1302203, Zhu JX) and National Natural Science
307 Foundation of China (31500937, Feng XY).

308 Conflicts of Interest: All the authors of the manuscript have read the journal's policy
309 on disclosure of potential conflicts of interest and agreed to its content. The
310 manuscript is original, has not already been published in any other journal and is not
311 currently under consideration by any another journal.

312 **REFERENCES**

- 313 ANDRSON G, NOORIAN AR, TAYLOR G, ANITHA M, BERNHARD D,
314 SRINIVASAN S, GREENE JG: Loss of enteric dopaminergic neurons and associated
315 changes in colon motility in an MPTP mouse model of Parkinson's disease. *Exp*
316 *Neurol* **207**:4-12, 2007.
- 317 ANSEMI L, TOTI L, BOVE C, TRAVAGLI RA: Vagally mediated effects of brain
318 stem dopamine on gastric tone and phasic contractions of the rat. *Am J Physiol*
319 *Gastrointest Liver Physiol* **313**(5):434-441, 2017.
- 320 BOIX J, PADEL T, PAUL G: A partial lesion model of Parkinson's disease in
321 mice-characterization of a 6-OHDA-induced medial forebrain bundle lesion. *Behav*
322 *Brain Res* **284**:196-206, 2015.
- 323 DEUMENS R, A BLOKLAND, PRICKAERTS J: Modeling Parkinson's disease in
324 rats: an evaluation of 6-OHDA lesions of the nigrostriatal pathway. *Exp Neurol* **175**
325 (2): 303-17, 2002.
- 326 DUTY S & JENNER P: Animal models of Parkinson's disease: a source of novel
327 treatments and clues to the cause of the disease. *Br J Pharmacol* **164** (4): 1357-1391,
328 2011.
- 329 FENG XY, LI Y, LI LS, LI XF, ZHENG LF, ZHANG XL, FAN RF, SONG J,
330 HONG F, ZHANG Y, ZHU JX: Dopamine D1 receptors mediate dopamine-induced
331 duodenal epithelial ion transport in rats. *Transl Res* **161**(6):486-494, 2013.
- 332 FENG XY, ZHANG DN, WANG YA, FAN RF, HONG F, ZHANG Y, LI Y, ZHU
333 JX: Dopamine enhances duodenal epithelial permeability via the dopamine D₅

334 receptor in rodent. *ACTA Physiologia (Oxf)*. **220**(1):113-123, 2017.

335 FERRO MM, BELLISSIMO MI, ANSELMO-FRANCI JA, ANGELLUCCI ME,
336 CANTERAS NS, DA CC: Comparison of bilaterally 6-OHDA- and MPTP-lesioned
337 rats as models of the early phase of Parkinson's disease: histological, neurochemical,
338 motor and memory alterations. *J Neurosci Methods* **148** (1): 78-87, 2005.

339 GRANDI LC, DI GIOVANNI G, GALATI S: Animal models of early-stage
340 Parkinson's disease and acute dopamine deficiency to study compensatory
341 neurodegenerative mechanisms. *J Neurosci Methods* **308**:205-218, 2018.

342 IMBRIANI P, SCIAMANNA G, SANTORO M, SCHIRINZI T, PISANI A:
343 Promising rodent models in Parkinson's disease. *Parkinsonism Relat Disord* **46** (1):
344 10-14, 2018.

345 JAKARIA M, PARK SY, HAQUE ME, KARTHIVASHAN G, KIM IS, GANESAN
346 P, CHOI DK: Neurotoxic Agent-Induced Injury in Neurodegenerative Disease Model:
347 Focus on Involvement of Glutamate Receptors. *Front Mol Neurosci* **11**:307, 2018.

348 JIANG P & DICKSON DW: Parkinson's disease: experimental models and reality.
349 *Acta Neuropathol* **135** (1): 13-32, 2018.

350 JOHNSON M E, LIM Y, SENTHILKUMARAN M, ZHOU XF, BOBROVSKAYA L:
351 Investigation of tyrosine hydroxylase and BDNF in a low-dose rotenone model of
352 Parkinson's disease. *J Chem Neuroanat* **70**: 33-41, 2015.

353 KIM HD, JEONG KH, JUNG UJ, KIM SR: Myricitrin ameliorates 6-hydroxy-
354 dopamine-induced dopaminergic neuronal loss in the substantia nigra of mouse brain.
355 *J Med Food* **19**:374-382, 2016.

356 MARIN C, BONASTRE M, MENGOD G, CORTES R, GIRALT A, OBESO JA,
357 SCHAPIRA AH: Early L-dopa, but not pramipexole, restores basal ganglia activity in
358 partially 6-OHDA-lesioned rats. *Neurobiol Dis* **64**: 36-47, 2014.

359 MARIN C, BONASTRE M, MENGOD G, CORTES R, RODRIGUEZ-OROZ MC:
360 From unilateral to bilateral parkinsonism: Effects of lateralization on dyskinesias and
361 associated molecular mechanisms. *Neuropharmacology* **97**: 365-75 ,2015.

362 MATTEO FORNAI, CAROLINA PELLEGRINI, LUCA ANTONIOLI, CRISTINA
363 SEGNANI, CHIARA IPPOLITO, ELISABETTA BAROCELLI, VIGILIO
364 BALLABENI, GAIA VEGEZZI, ZAINAB AI HARRAQ, FABIO BLANDINI,
365 GIOVANNA LEVANDIS, SILVIA CERRI, CORRADO BLANDIZZI, NUNZIA
366 BERNARDINI, ROCCHINA COLUCCI: Enteric dysfunctions in experimental
367 Parkinson's disease: alterations of excitatory cholinergic neurotransmission regulating
368 colonic motility in rats. *J Pharmacol Exp Ther* **356**:434-444, 2016.

369 CAROLINA PELLEGRINI[#], MATTEO FORNAI^{*#}, ROCCHINA COLUCCI, ERIKA
370 TIROTTA, FABIO BLANDINI, GIOVANNA LEVANDIS, SILVIA CERRI,
371 CRISTINA SEGNANI, CHIARA IPPOLITO: Alteration of colonic excitatory
372 tachykininergic motility and enteric inflammation following dopaminergic
373 nigrostriatal neurodegeneration. *Journal of Neuroinflammation* **13**:146, 2016.

374 MONICA VT, ELLEN GC, VERA C, CAROLINE L, SIV A, OLE H TINE RL,
375 MARTIN IB: Antibiotic treatment affects intestinal permeability and gut microbial
376 composition in Wistar rats dependent on antibiotic class. *PLOS one* **10**(12):0144854,
377 2015.

378 MOUSSAOUI N, LARAUCHE M, BIRAUD M, MOLET J, MILLION M, MAYER
379 E, TACHE Y: Limited Nesting Stress Alters Maternal Behavior and In Vivo Intestinal
380 Permeability in Male Wistar Pup Rats. *PLoS One* **11**(5): 0155037, 2016.

381 NATALE G, KASTSIUSHENKA O, FULCERI F, RUGGIERI S, PAPARELLI A,
382 FORNAI F: MPTP-induced parkinsonism extends to a subclass of TH-positive
383 neurons in the gut. *Brain Res* **1355**: 195-206, 2010.

384 NETUSHA T, ALICJA P, CHRISTIAN S, AVEE N, SZAMOSI JC, CHRIS PV,
385 DESSI L, LOUIS PS, JENNIFER J, KEVIN PF, JONATHAN DS, MAGGIE JL,
386 DONALD JD, ELENA FV, MICHAEL GS, DAWN MEB: Age-Associated Microbial
387 Dysbiosis Promotes Intestinal Permeability, Systemic Inflammation, and Macrophage
388 Dysfunction. *Cell Host Microbe* **21**(4): 455-466, 2017.

389 ODIN P[#], CHAUDHURI KR[#], VOLKMANN J, ANTONINI A, STORCH A,
390 DIETRICH E, PIROSEK Z, HENRIKSEN T, HORNE M, DEVOS D,
391 BERGQUIST F: Viewpoint and practical recommendations from a movement
392 disorder specialist panel on objective measurement in the clinical management of
393 Parkinson's disease. *NPJ Parkinsons Dis* **4**:14, 2018.

394 SAUERBIER A, JITKRITSADAKUL O, TITOVA N, KLINGELHOEFER L,
395 TSUBOI Y, CARR H, KUMAR H, BANERJEE R, ERRO R, BHIDAYASIRI R,
396 SCHRAG A, ZIS P, LIM SY, AL-HASHEL JY, KAMEL WA, MARTINEZ
397 MARTIN P, RAYY CHAUDHURI K: Non-Motor Symptoms Assessed by
398 Non-Motor Symptoms Questionnaire and Non-Motor Symptoms Scale in Parkinson's
399 Disease in Selected Asian Populations. *Neuroepidemiology* **49**(1-2):1-17, 2017.

400 SCHNEIDER JS, PIOLI EY, JIANZHONG Y, LI Q, BEZARD E: Levodopa
401 improves motor deficits but can further disrupt cognition in a macaque Parkinson
402 model. *Mov Disord* **28** (5): 663-667, 2013.

403 SHEN DF, TIAN XY, ZHANG BB, SONG RR: Mechanistic evaluation of
404 neuroprotective effect of estradiol on rotenone and 6-OHDA induced Parkinson's
405 disease. *Pharmacological Reports* **69**(6):1178-1185, 2017.

406 SHIREEN E, PERVEZ S, MASROOR M, ALI WB, RAIS Q, KHALIL S, TARIQ A,
407 HALEEM DJ: Reversal of haloperidol induced motor deficits in rats exposed to
408 repeated immobilization stress. *Pak J Pharm Sci* **27** (5): 1459-1466, 2014.

409 STEWARD MC, ISHIGURO H, CASE RM: Mechanisms of bicarbonate secretion in
410 the pancreatic duct. *Annu Rev Physiol* **67**:377-409, 2005.

411 SUN M, HE C, CONG Y, LIU Z: Regulatory immune cells in regulation of intestinal
412 inflammatory response to microbiota. *Mucosal Immunol* **8**(5): 969-978, 2015.

413 TIAN YM, CHEN X, LUO DZ, ZHANG XH, XUE H, ZHENG LF, YANG N,
414 WANG, XM, ZHU JX: Alteration of dopaminergic markers in gastrointestinal tract of
415 different rodent models of Parkinson's disease. *Neuroscience* **153**: 634-644, 2008.

416 ZHANG XL, LI Y, LIU CZ, FAN RF, WANG P, ZHENG LF, HONG F, FENG XY,
417 ZHANG Y, LI LS, ZHU JX: Alteration of enteric monoamines with monoamine
418 receptors and colonic dysmotility in 6-hydroxydopamine induced Parkinson's disease
419 rats. *Transl Res* **66**(2):152-162, 2015.

420 ZHENG LF, SONG J, FAN RF, CHEN CL., REN QZ, ZHANG X L, FENG XY,
421 ZHANG Y, LI LS, ZHU JX: The role of the vagal pathway and gastric dopamine in

422 the gastroparesis of rats after a 6-hydroxydopamine microinjection in the substantia
423 nigra. *Acta Physiologica* **211**(2): 434-46, 2014.

424 ZHENG LF, WANG ZY, LI XF, SONG J, HONG F, LIAN H, WANG Q, FENG XY,
425 TANG YY, ZHANG Y, ZHU JX: Reduced expression of choline acetyltransferase in
426 vagal motoneurons and gastric motor dysfunction in a 6-OHDA rat model of
427 Parkinson's disease. *Brain Res* **1420**: 59-67, 2011.

428 ZHENG Z & TRAVAGLI RA: Dopamine effects on identified rat vagal motoneurons.
429 *Am J Physiol Gastrointest Liver Physiol* **292**, 1002-1008, 2007.

430 ZIS P, ERRO R, WALTON CC, SAUERBIER A, CHAUDHURI KR: The range and
431 nature of non-motor symptoms in drug-naive Parkinson's disease patients: a
432 state-of-the-art systematic review. *Nature Parkinson's Journal (NPJ) Parkinson's*
433 *disease* **1**:15013, 2015.

434 **FIGURES WITH CAPTIONS**

435 **Fig. 1.** Characterization of bilateral 6-OHDA lesions.

436 (A&B) The TH immunoreactivity and DA content in the SNs and striata of control
437 and 6-OHDA rats. (C) The rotarod test results of control and 6-OHDA rats. (D) The
438 original recording showing daily food debris of control and 6-OHDA rats. (E) A
439 summary of the daily food debris of the control and 6-OHDA rats. Values are the
440 means \pm S.E.M. * $p < 0.05$, ** $p < 0.01$, and *** $p < 0.001$

441 **Fig. 2.** Gastrointestinal motility dysfunction of the 6-OHDA rats.

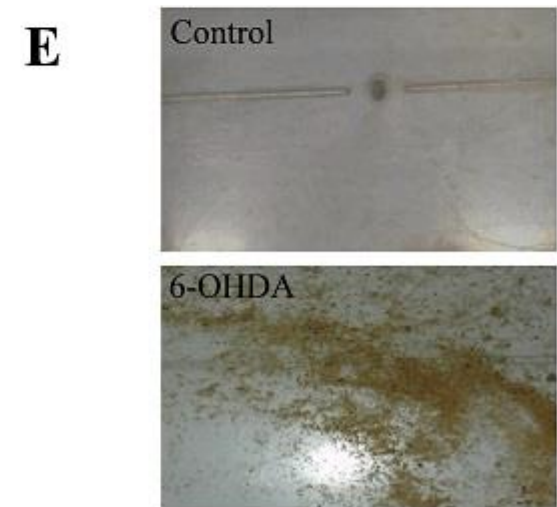
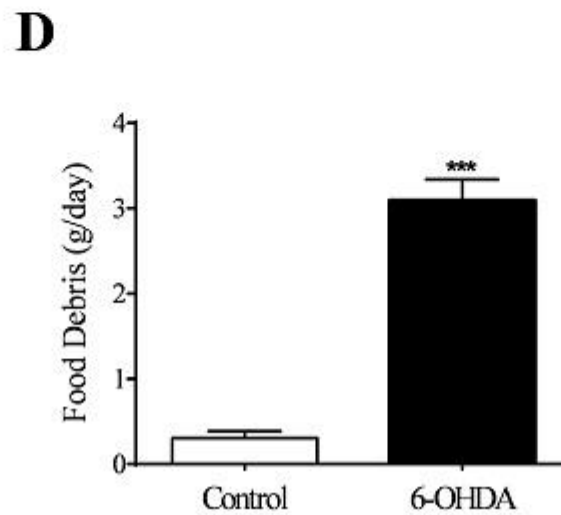
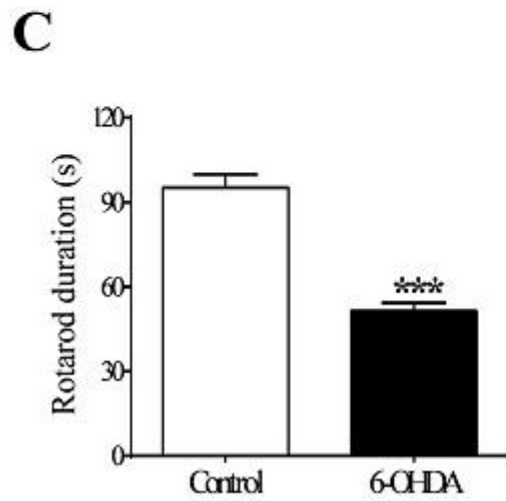
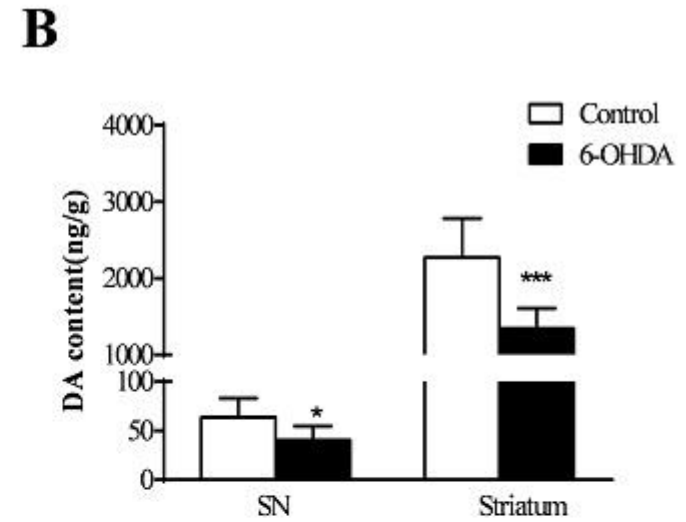
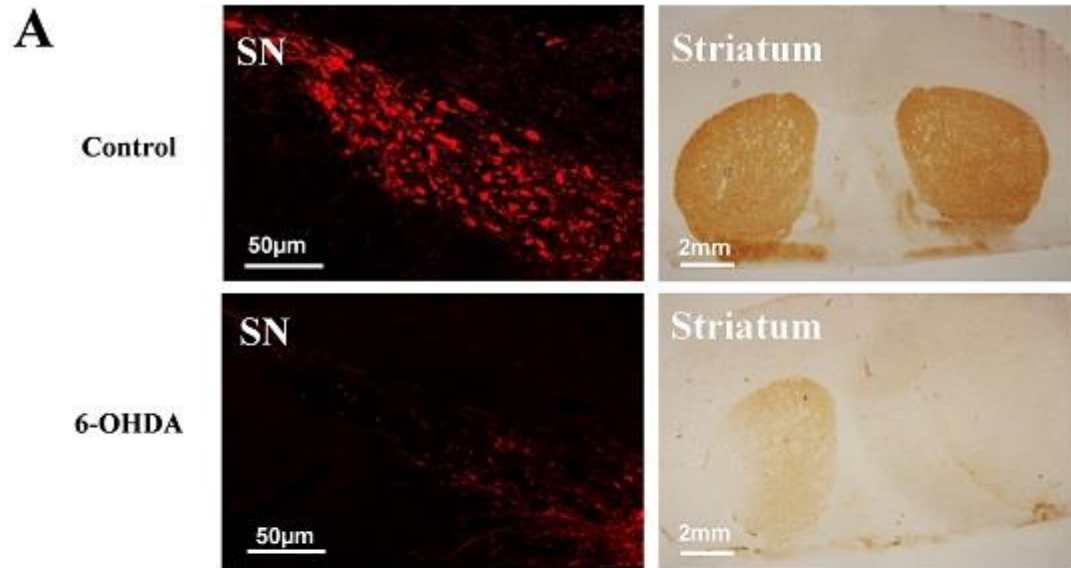
442 (A) The original images of gastric emptying every 45 min after barium meal ingestion
443 in control and 6-OHDA rats. (B) The gastric area and emptying of the barium meal

444 after 3 h in control and 6-OHDA rats. (C) The total intestinal transit time in control
445 and 6-OHDA rats. (D-F) The number of stools and solid matter and moisture content
446 of faeces in control and 6-OHDA rats. Values are means \pm S.E.M. * p <0.05, ** p <0.01,
447 and *** p <0.001.

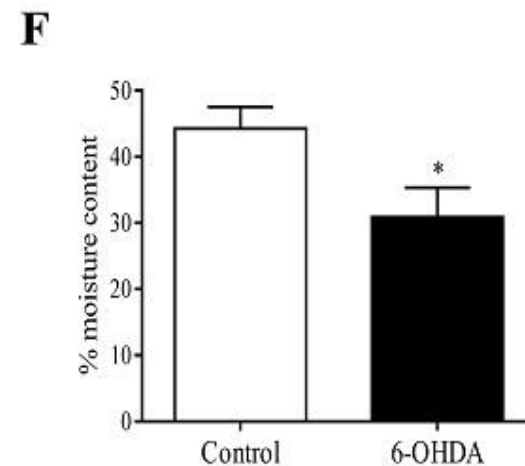
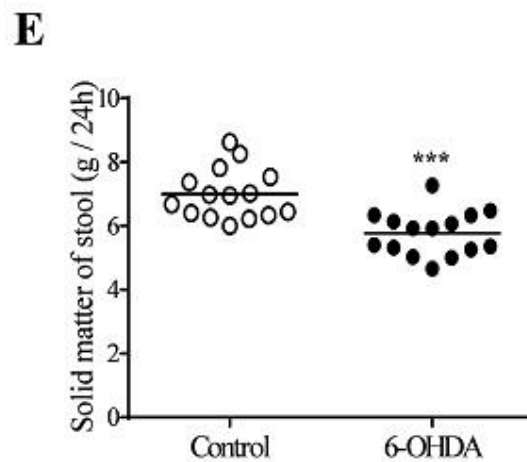
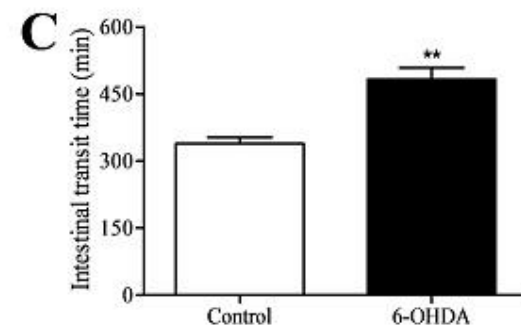
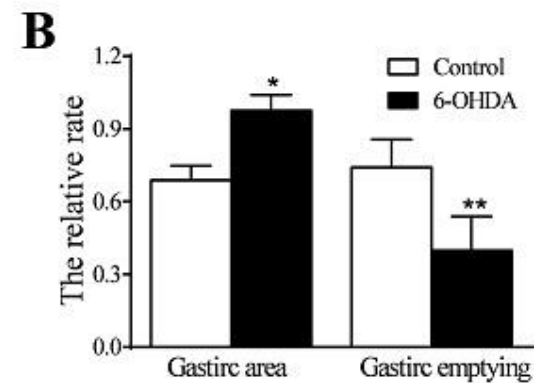
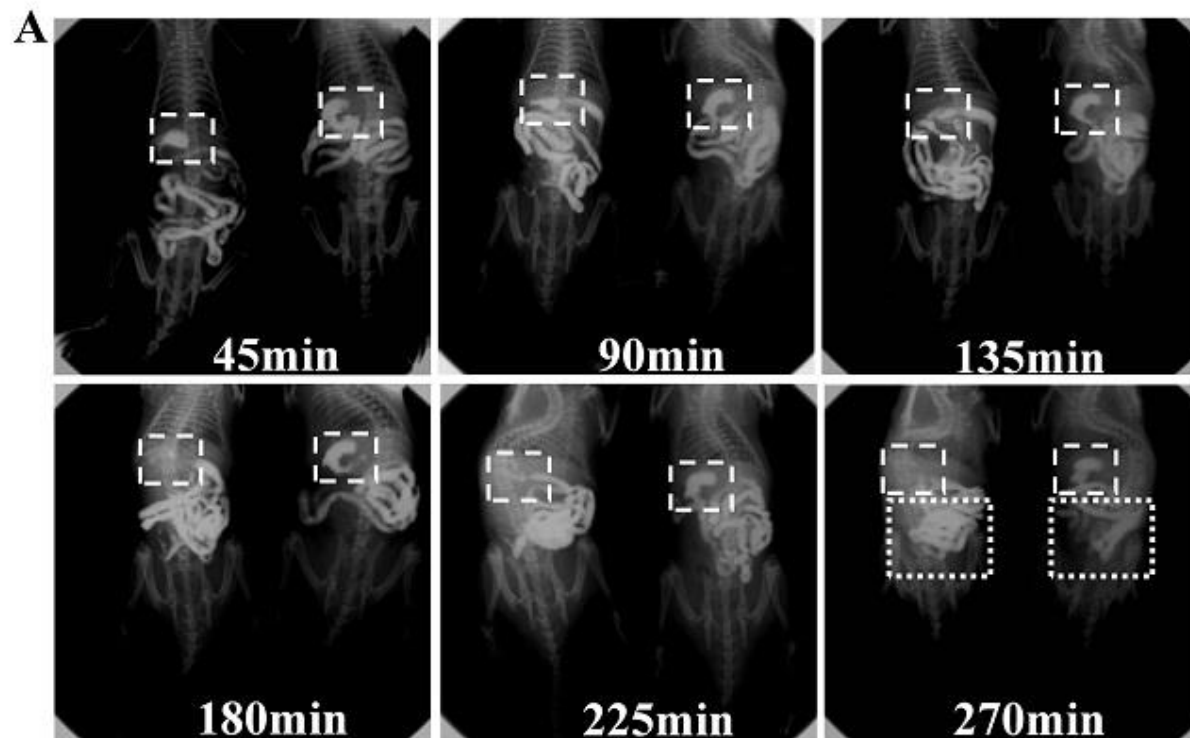
448 **Fig. 3.** Gastrointestinal barrier dysfunction of the 6-OHDA rats.

449 (A) The FITC-dextran concentration in the plasma of control and 6-OHDA rats. (B)
450 The TERs of duodenal and colonic preparations in the control and 6-OHDA rats. (C)
451 The inflammatory factors in the plasma of control and 6-OHDA rats. Values are
452 means \pm S.E.M. * p <0.05, ** p <0.01, and *** p <0.001.

Figures. 1

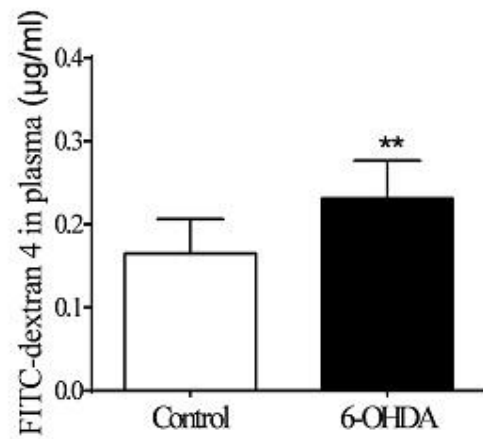


Figures. 2

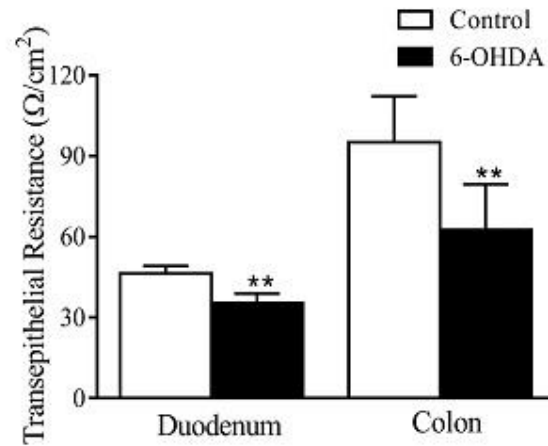


Figures. 3

A



B



C

